Numerical Simulations of Hydrodynamic Behaviors in Conical Spouted Beds

Z.G. Wang, H.T. Bi and C.J. Lim

Fluidization Research Centre

Department of Chemical and Biological Engineering

University of British Columbia

Vancouver, BC, V6T 1Z4, Canada

Abstract

By comparison with experimental data on the radial distribution of the static pressure and vertical particle velocity in conical spouted beds, numerical simulations show that, among all factors investigated, the axial solid phase source term has the most significant influence on static pressure profiles, followed by the restitution coefficient, while other factors almost have no effect. Apart from the solid bulk viscosity, almost all other factors affect the radial distribution of the axial particle velocity, although the influence of the axial solid phase source term is less significant. For complex systems such as conical spouted beds, the new approach proposed in this work by properly selecting the axial solid phase source term shows a great potential to improve the CFD simulation of spouted beds.

Keywords: Conical spouted bed; Hydrodynamics; Numerical simulation; Multiphase model

1. Introduction

Due to the vigorous solids motion and intimate gas-solids contact, conical spouted beds have been commonly used for drying suspensions, solutions and pasty materials (Pham, 1983; Markowski, 1992; Passos et al., 1997, 1998; Reyes et al., 1998). Many other applications have also been under research and development, such as catalytic partial oxidation of methane to produce synthesis gas (Marnasidou et al., 1999), incineration of waste-materials, coating of medical tablets (Kucharski & Kmiec, 1983), coal gasification and liquefaction (Uemaki & Tsuji, 1986), pyrolysis of sawdust or mixtures of wood residues (Aguado et al., 2000a, 2000b; Olazar et al., 2000a, 2000b, 2001).

Comparing with other multiphase systems, such as fixed beds or packed beds, fluidized beds, circulating fluidized beds (co-current upflow) and co-current downflow fluidized beds (downer), numerical simulations of spouted beds, especially conical spouted beds, have received less attention and reported results are still insufficient and controversial. Duarte et al. (2005) simulated a cylindrical spouted bed as described by He ea al. (1994a, 1994b). In their simulation, the parabolic velocity profile which is typical for the laminar flow was used as the turbulent inlet boundary condition, and the average velocity used was higher than the actual operating condition. By using empirical correlations for granular viscosity (originally obtained from experiments for FCC particles) and elasticity modulus, Huilin et al. (2001) and He et al. (2004) simulated experiments of He et al. (1994a, 1994b). Huilin et al. (2001) also simulated experiments for a conical spouted bed operated by San Jose et al. (1998). Based on their

descriptions, the uniform velocity profile was applied for the turbulent inlet boundary condition. Taking the kinetic theory approach for granular flow, Lu et al. (2004) simulated experiments of He et al. (1994a, 1994b) for cylindrical spouted beds and experiments of San Jose et al. (1998) for a conical spouted bed, with the uniform velocity profile applied for the turbulent inlet boundary condition. Kawaguchi et al. (2000) simulated experiments of He et al. (1994b) too. In their simulation, particle motion was treated discretely by solving Newton's equation of motion for each particle, the discrete element method (DEM) was employed to model the interaction between particles, with a uniform velocity profile applied to the inlet.

It is well known that, for a cylindrical multiphase system, as the fluid velocity is increased, the pressure drop across the bed increases before the minimum fluidization velocity is reached, and the multiphase system is operated as a packed bed or fixed bed with the pressure drop of the bed being well described by the Ergun equation. Once the minimum fluidization velocity has been achieved, particles are in a dynamically suspended condition, and the pressure drop across the bed will remain constant within a wide range of fluid velocity, being equal to the effective weight of the bed per unit area. Because of the difference of the suspended state between a packed bed and a fluidized bed, approaches used to simulate packed beds and fluidized beds are quite different. For example, there are two options in commercial software FLUENT specially designed for simulating packed beds.

For spouted beds, the bed structure is quite different from conventional fluidized beds and packed beds. At stable spouting, a spouted bed consists of three regions, a spout in the center, a fountain above the bed surface and an annulus between the spout and the wall. The spout and the fountain are similar to fluidized beds with particles dynamically suspended, while the annulus region is more like a packed bed or moving bed. At partial spouting, there are only two distinct regions, an internal spout that is similar to a fluidized bed and the surrounding packed particle region which is similar to a packed bed. Thus, original codes used for simulating fluidized beds or packed beds in commercial softwares are unsuitable for the simulation of spouted beds. Furthermore, at stable spouting, it was found that the maximum ratio of the spouting to the fluidization pressure drop is about 0.64-0.75 for cylindrical spouted beds (Mathur and Epstein, 1974); for conical spouted beds, the ratio of the spouting to the fluidization pressure drop is about 0.4 based on our recent experimental data as well as those from Mukhlenov and Groshtein (1964, 1965), well below the pressure drop under fluidized conditions. This suggests that particles are not in fully suspended state even at stable spouting, the inclined wall as well as the base of the bed exert some kind of supporting forces on particles in the upper region. From this point of view, for spouted beds, the general gravity term in the vertical momentum equation for the granular phase in commercial software for simulating fluidized beds seems to be not applicable, and thus needs to be modified.

For conical spouted beds, because of the existence of the inclined wall, the radial momentum equation for the granular phase should also be modified. For cylindrical spouted beds, if the static bed height is higher enough, the conical base takes only a small part of the whole bed, and the modification of the radial momentum equation can be neglected. Whereas, considering the complexity of the flow structure of conical spouted beds, we only focus on the vertical momentum equation for granular phase in the annulus in the current simulation.

Several studies have been reported on the effect of factors on simulation results of gas-solids fluidized beds. Goldschmidt et al. (2001) reported that the hydrodynamics of dense

gas-fluidized beds strongly depends on the amount of energy dissipated due to particle collisions or the restitution coefficient. McKeen and Pugsley (2003) simulated a freely bubbling bed of fluid catalytic cracking (FCC) catalyst using four kinds of drag models, and found that the same degree of bed expansion was achieved using different drag equations. Therefore, they concluded that simply choosing a different drag model could not improve predictions, and a modified drag model by introducing a scale factor had to be applied in their simulations in order to bring their simulation result close to their experimental data. They also investigated the effect of the mesh size on simulation results. Yang et al. (2003) simulated a circulating fluidized bed using both the Gidaspow drag model and a modified Gidaspow drag model based on a new voidage function derived from their EMMS (the Energy-Minimization Multi-Scale) approach. It was found that the dynamic formation and dissolution of clusters could be captured using their modified drag model, with the simulated outlet solid flux and voidage profile in both radial and axial directions being in reasonable agreement with experimental results. Lu et al. (2004) investigated the effect of the restitution coefficient and the frictional viscosity in their simulation of San Jose et al. (1998) experimental data. It was shown that both the restitution coefficient and the frictional viscosity had effects on the radial voidage distribution to some extent.

The objective of this study is to investigate the effects of those factors, especially the solids phase source term, on CFD simulation results of a conical spouted bed at stable spouting state. In the simulation, the fluidized beds approach is used with user-defined functions (UDFs) to modify different gravity terms in the annulus region, different fluid inlet profiles and different fluid-solid exchange coefficients. Experimental data on the distribution of the static pressure, vertical solid velocity, and solid fraction are then used to validate simulation results.

2. Governing Equations

Currently there are two approaches for the numerical calculation of multiphase flows: the Euler-Lagrange approach and the Euler-Euler approach.

In the Euler-Lagrange approach, the fluid phase is treated as a continuum by solving the time averaged Navier-Stokes equations, while the dispersed phase is solved by tracking a large number of particles (or bubbles, droplets) through the calculated flow field. The dispersed phase can exchange momentum, mass, and energy with the fluid phase. A fundamental assumption made in this approach is that the dispersed second phase occupies a low volume fraction.

In the Euler-Euler approach, the different phases are treated mathematically as interpenetrating continua. Since the volume of a phase cannot be occupied by the other phases, the concept of phasic volume fraction is introduced. These volume fractions are assumed to be continuous functions of space and time and their sum is equal to one.

In FLUENT, three different Euler-Euler multiphase models are available. For granular flows, such as flows in risers, fluidized beds and other suspension systems, the Eulerian multiphase model is always the first choice, so does our simulation on gas-solid conical spouted beds.

Based on the general description of the Eulerian multiphase model, by simplification, following governing equations can be derived.

Assumptions:

- No mass transfer between spouting gas and glass bead particles;
- External body force, lift force, as well as virtual mass force are ignored;
- Density of each phase is a constant.

Continuity equation for phase *q* (both fluid phase *l* and solid phase *s*):

$$\frac{\partial}{\partial t}(\alpha_q)+\nabla\cdot(\alpha_q\vec{v}_q)=0 \tag{1}$$

where $\vec{v}_q$ is the velocity of phase *q*; α_q is the volume fraction of phase *q*, and the following condition holds.

$$\sum_{q=1}^{n}\alpha_q=1 \tag{2}$$

where *n* is the total number of phases, and *n*=2 in our simulation.

Conservation equation of momentum:

For the fluid phase *l*:

$$\frac{\partial}{\partial t}(\alpha_l\rho_l\vec{v}_l)+\nabla\cdot(\alpha_l\rho_l\vec{v}_l\vec{v}_l)=-\alpha_l\nabla P+\nabla\cdot\bar{\bar{\tau}}_l+\alpha_l\rho_l\vec{g}+K_{sl}(\vec{v}_s-\vec{v}_l) \tag{3}$$

For the solid phase *s*:

$$\frac{\partial}{\partial t}(\alpha_s\rho_s\vec{v}_s)+\nabla\cdot(\alpha_s\rho_s\vec{v}_s\vec{v}_s)=-\alpha_s\nabla P-\nabla P_s+\nabla\cdot\bar{\bar{\tau}}_s+\alpha_s\rho_s\vec{g}+K_{ls}(\vec{v}_l-\vec{v}_s)+\vec{S}_s \tag{4}$$

where ρ_l is the density of the fluid phase, *P* is the static pressure shared by all phases, $\bar{\bar{\tau}}_l$ is the fluid phase stress-strain tensor, $\vec{g}$ is the gravitational acceleration, $K_{ls}=K_{sl}$ is the momentum exchange coefficient between fluid phase *l* and solid phase *s*, ρ_s is the density of the particle, $\bar{\bar{\tau}}_s$ is the solid phase stress-strain tensor, P_s is the solid pressure, $\vec{S}_s$ is the solid phase source term.

The stress-strain tensor for phase *q*:

$$\bar{\bar{\tau}}_q=\alpha_q\mu_q(\nabla\vec{v}_q+\nabla\vec{v}_q^{T})+\alpha_q(\lambda_q-\frac{2}{3}\mu_q)\nabla\cdot\vec{v}_q\bar{\bar{I}} \tag{5}$$

where μ_q and λ_q are the shear and bulk viscosity of phase q.

For the solid phase s, the solids shear viscosity is the sum of the collisional viscosity, kinetic viscosity and the optional frictional viscosity, as shown in equation (6).

$$\mu_s = \mu_{s,col} + \mu_{s,kin} + \mu_{s,fr} \tag{6}$$

The collision viscosity is modeled as:

$$\mu_{s,col} = \frac{4}{5}\alpha_s \rho_s d_s g_{0,ss}(1+e_{ss})\left(\frac{\Theta_s}{\pi}\right)^{1/2} \tag{7}$$

where d_s is the diameter of the solid particles, $g_{0,ss}$ is the radial distribution function, and FLUENT employs the following expression as equation (8), e_{ss} is the coefficient of restitution, Θ_s is the granular temperature.

$$g_{0,ss} = \left[1 - \left(\frac{\alpha_s}{\alpha_{s,\max}}\right)^{1/3}\right]^{-1} \tag{8}$$

The following expression from Gidaspow (1994) is used to estimate the kinetic viscosity.

$$\mu_{s,kin} = \frac{10\rho_s d_s \sqrt{\Theta_s \pi}}{96\alpha_s (1+e_{ss}) g_{0,ss}}\left[1 + \frac{4}{5} g_{0,ss}\alpha_s (1+e_{ss})\right]^2 \tag{9}$$

In our simulation, the frictional viscosity was not considered, and the solid bulk viscosity used either the following form from Lun et al. (1984) or a constant value of zero.

$$\lambda_s = \frac{4}{3}\alpha_s \rho_s d_s g_{0,ss}(1+e_{ss})\left(\frac{\Theta_s}{\pi}\right)^{1/2} \tag{10}$$

Fluid-solid exchange coefficients:

The fluid-solid exchange coefficient K_{sl} can be written in the following general form:

$$K_{sl} = \frac{\alpha_s \rho_s f}{\tau_s} \tag{11}$$

where f is defined differently for the different exchange coefficient models, and τ_s, the "particulate relaxation time", is defined as

$$\tau_s = \frac{\rho_s d_s^2}{18\mu_l} \tag{12}$$

In FLUENT, there are three models for fluid-solid exchange coefficient, and the Gidaspow drag model is applied in this work.

Gidaspow drag model (1994):

The Gidaspow model is a combination of the Wen and Yu model (1966) and the Ergun (1952) equation.

When $\alpha_l > 0.8$, the fluid-solid exchange coefficient K_{sl} is of the following form:

$$K_{sl} = \frac{3}{4} C_D \frac{\alpha_s \alpha_l \rho_l |\vec{v}_s - \vec{v}_l|}{d_s} \alpha_l^{-2.65} \tag{13}$$

where, $C_D = \frac{24}{\alpha_l \mathrm{Re}_s} \left[1 + 0.15(\alpha_l \mathrm{Re}_s)^{0.687}\right]$ (14)

$$\mathrm{Re}_s = \frac{\rho_l d_s |\vec{v}_s - \vec{v}_l|}{\mu_l} \tag{15}$$

When $\alpha_l \leq 0.8$

$$K_{sl} = 150 \frac{\alpha_s (1-\alpha_l) \mu_l}{\alpha_l d_s^2} + 1.75 \frac{\rho_l \alpha_s |\vec{v}_s - \vec{v}_l|}{d_s} \tag{16}$$

Solids Pressure:

For granular flows in the compressible regime (i.e., where the solids volume fraction is less than its maximum allowed value), a solids pressure is calculated independently and used for the pressure gradient term, ∇P_s, in the solid phase momentum equation. The solids pressure is composed of a kinetic term and a second term due to particle collisions, as shown in equation (17) (Fluent Inc., 2003b).

$$P_s = \alpha_s \rho_s \Theta_s + 2\rho_s (1 + e_{ss}) \alpha_s^2 g_{0,ss} \Theta_s \tag{17}$$

The solid phase source term:

It was found that the ratio of the pressure drop at stable spouting to the pressure drop at stable fluidization is usually smaller than one for both the cylindrical spouted beds and the conical spouted beds (Mathur and Epstein, 1974; Mukhlenov and Groshtein, 1964, 1965). At partial spouting state, however, the above ratio is usually bigger than one in the ascending process. Thus, the gravity term in the axial solid phase momentum equation, equation (4), needs to be modified. To do so, a solid phase source term, $S_{s,a}$, is introduced into the axial solid phase momentum equation for both the spout and annulus regions:

When $\alpha_l \leq 0.8$ and $Z \leq H_0$ (in the annulus)

$$S_{s,a} = -\alpha_s \rho_s g + k_a(\alpha_s \rho_s g) = (k_a - 1)\alpha_s \rho_s g \quad (18)$$

When $\alpha_l > 0.8$ (in the spout and the fountain)

$$S_{s,a} = -\alpha_s \rho_s g + k_s(\alpha_s \rho_s g) = (k_s - 1)\alpha_s \rho_s g \quad (19)$$

where Z is the axial height, H_0 is the static bed height, k_a and k_s are the ratio of the pressure drop of spouted beds to the pressure drop at stable fluidization, which are functions of operating conditions and the geometrical structure of the bed. In the gas velocity ascending process, when the spouted bed is operated at partial spouting state, k_a is usually greater than one. To simplify the problem, k_s was usually set to one.

By applying the above solid phase source term, it is possible to use FLUENT to simulate a spouted bed operated at partial spouting or stable spouting state for both the ascending and the descending processes.

3. Simulating Conditions

Table 1. List of simulation conditions

Description	Value	Comment
Operating gas velocity, U_i	24 m/s	Based on D_i
Gas density, ρ_l	1.225 kg/m^3	Air
Gas viscosity, μ_l	1.7894×10^{-5} kg/(m·s)	Air
Particle density, ρ_s	2500 kg/m^3	Spherical glass beads
Particle diameter, d_s	0.00116 m	Uniform distribution
Initial solid packing, $\alpha_{s,0}$	0.61	Fixed value
Packing limit, $\alpha_{s,max}$	0.61	Fixed value
Solid viscosity, μ_s	Gidaspow	Eq. (7) + Eq. (9)
Solid bulk viscosity (Base case), λ_s	0	Fixed value
Cone angle, γ	45°	Fixed value
Diameter of the upper section, D_c	0.45 m	Fixed value
Total height of the column	1.6 m	Fixed value
Gas inlet diameter, D_0	0.019 m	Fixed value
Diameter of the bed bottom, D_i	0.038 m	Fixed value
Static bed height, H_0	0.396 m	Fixed value
Solver	2 dimensional, double precision, segregated, unsteady, 1st order implicit, axisymmetric	
Multiphase Model	Eulerian Model, 2 phases	
Viscous Model	Laminar model	
Phase Interaction (Base case)	Fluid-solid exchange coefficient: Gidaspow Model Restitution coefficient: 0.9	
Time steps (Final value)	0.00001s	Fixed value
Convergence criterion	10^{-3}	Default in FLUENT

Table 2. Boundary conditions

Description	Comment
Inlet	Three types of radial distributions are tested for fluid phase
	No particles enter for solid phase
Outlet	Uniform velocity distribution for fluid phase
	No particle exits for solid phase
Axis	Axisymmetric
Wall	Non-slip for fluid phase
	Zero shear stress for solid phase

In the simulation, the bed geometrical structure and dimensions (as shown in Fig. 1 (b)), the spouting gas, the bed material as well as operating conditions used are kept almost the same as in the actual experiment. The operating gas velocity used in simulations is about 2% higher than the experiment, and the total column height is much longer than the actual experimental setup. Because of the influence of the outlet structure on flow field, comparisons between the experiment and simulation will not be considered above the bed surface. Details on simulation conditions are listed in Table 1, with boundary conditions given in Table 2.

In order to investigate all possible factors that may affect simulation results, parameters such as the fluid inlet velocity profile, solid bulk viscosity, restitution coefficient, exchange coefficient and the source term are selected for the sensitivity analysis. At the same time, three kinds of mesh/grid partitions of the bed are also studied. All conditions investigated are summarized in Table 3.

Table 3. Summary of conditions used for sensitivity analysis

Grid Partition	Fluid Inlet Radial Profile	Bulk Viscosity	Restitution Coefficient	Exchange Coefficient	Source Term
Partition 1 (10497 cells)	Uniform	0	0.9	K_{sl} (Gidaspow)	k_a=1.0
	Parabolic				
	1/7th power law				
		Lun et al.			
		0	0.81		
			0.99		
			0.9	0.8* K_{sl} (Gidaspow)	
				1.2* K_{sl} (Gidaspow)	
				K_{sl} (Gidaspow)	k_a=0.7
					k_a=0.5
					k_a= k_s=0.5
					k_a=0.41
Partition 2 (4102 cells)					k_a=1.0
					k_a=0.7
					k_a=0.5
Partition 3 (2598 cells)					k_a=1.0
					k_a=0.7
					k_a=0.5

Notes: a. In simulations, k_s equals to1.0 unless having further indications;

b. Conditions for the base case are as follows: partition 1; parabolic fluid inlet profile; zero value of the solid bulk viscosity; restitution coefficient equals to 0.9; fluid-solid exchange coefficient estimated by the Gidaspow model, k_a equals to1.0.

4. Experiments

Experiment was conducted in two conical spouted to generate data for the validation of the simulation results. A schematic diagram of the experimental unit is shown in Fig. 1 (a). Conical spouted beds (both a semi-circular half column and a full column) are made of Plexiglas with an included angle γ of 45°. The diameter at the conical base D_i is 0.038 m, the diameter of the nozzle D_0 is 0.019 m, and the diameter of the upper cylindrical section D_c is 0.45 m. Glass beads of 0.00116 m in diameter were used as the bed material, compressed air at the ambient temperature was used as the spouting gas. Other particle properties and detailed operating conditions are shown in Table 4.

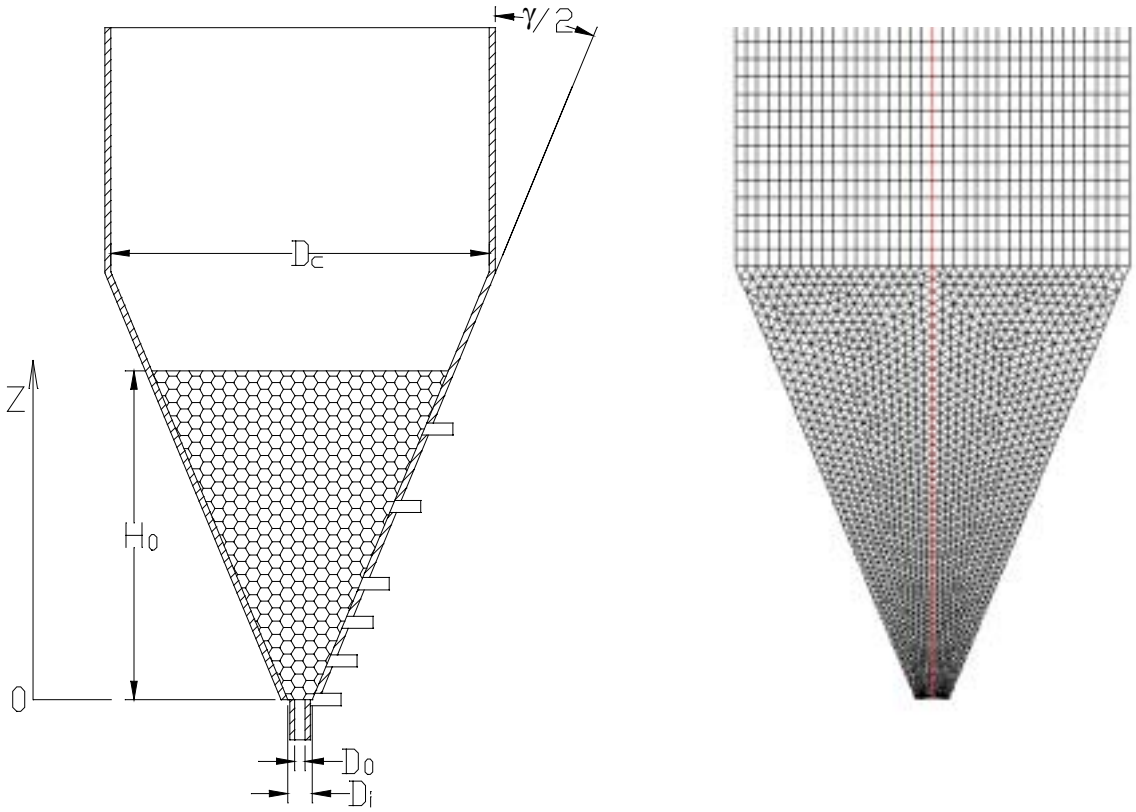

(a) (b)

Fig. 1. Schematic drawing of the Plexiglas conical spouted bed unit.

Table 4. Particle properties and operating conditions

Particle diameter d_s, (m)	Particle density ρ_s, (kg/m^3)	Lose-packed voidage, $\alpha_{l,0}$	Geldart's classification	Static bed height H_0, (m)	Velocity U_i, (m/s)
0.00116	2500	0.39	D	0.396	23.5

The distribution of the static pressure was measured by static pressure probes connected to differential pressure transducers; the distribution of the vertical solid velocity and solid hold up were measured by optical fiber probes which were calibrated separately in advance. During experiments, all probes can be radially traversed to measure the profile at each vertical position.

5. Results and Discussion

Notes for Fig. 2 to Fig. 7:

Figure (a)	Figure (b)
Red lines: Z=38mm; Blue lines: Z=89mm; Magenta lines: Z=191mm; Cyan lines: Z=292mm	Red lines: Z=140mm; Blue lines: Z=241mm Magenta lines: Z=343mm

The grid partition

The effect of grid size or grid partition on the simulation results is first examined by comparing the simulation results from three grid sizes. As shown in Figure 2, the grid size within the range investigated in the current simulation has little effect on the radial distribution of the static pressure, although some influence on the distribution of the axial solid velocity is observed, especially in the spout region. Thus, the more accurate grid partition with the smallest grid size, partition 1, was used in the following sensitivity analysis. It is also seen from Fig. 2 that simulated results on the axial solid velocity agree very well with experimental data, but not for the static pressure profile under the base operating conditions without the consideration of the solid phase source term.

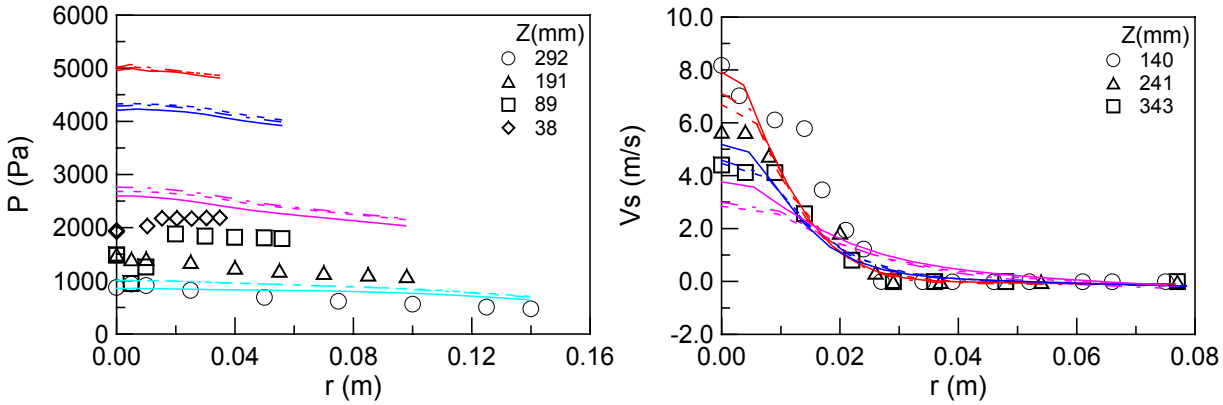

Fig. 2. Comparison between experimental results and simulated results with different grid partitions at k_a=1.0 (k_s=1.0, 1/7th power law). Symbols are experimental results, and lines are simulated results. (Solid lines correspond to partition 1, dotted dash lines correspond to partition 2, dash lines correspond to partition 3.)

The fluid inlet profile

The influence of fluid inlet profiles on the simulation result is shown in Fig. 3. Although fluid inlet profiles have little effect on the distribution of the static pressure, the influence on the distribution of the axial solid velocity is shown clearly, especially in the spout region. Simulated

static pressures overestimated experimental data significantly when k_a was chosen to be equal to 1.0, although the simulated particle velocity profile is quite close to the experimental data except for the case when a parabolic inlet gas velocity profile was used. Therefore, 1/7th power law or turbulent distribution inlet velocity profile was used in subsequent simulations.

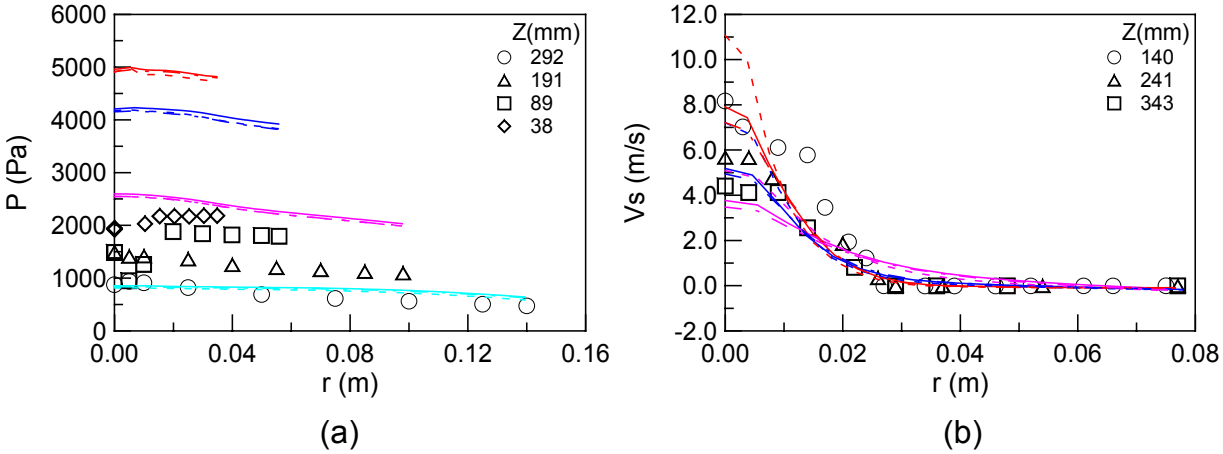

Fig. 3. Comparison between experimental results and simulated results with different fluid inlet profiles at k_a=1.0 (k_s=1.0). Symbols are experimental results, and lines are simulated results. (Solid lines correspond to the 1/7th power law or turbulent flow, dashed lines correspond to the parabolic profile or laminar flow, dotted dash lines correspond to the uniform profile.)

The solid bulk viscosity

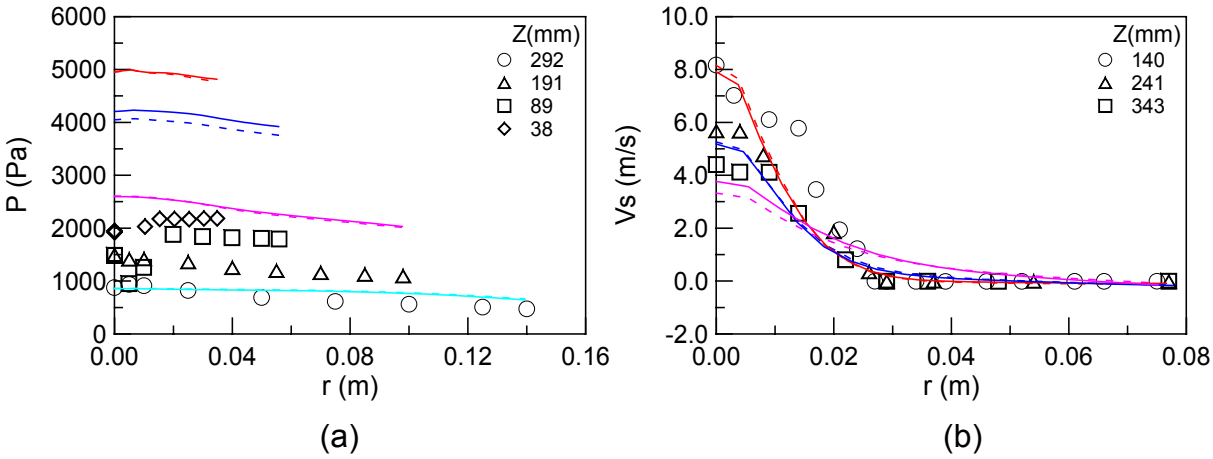

Fig. 4. Comparison between experimental results and simulated results with different solid bulk viscosity at k_a=1.0 (k_s=1.0, 1/7th power law). Symbols are experimental results, and lines are simulated results. (Solid lines correspond to zero value for the solid bulk viscosity, dashed lines correspond to the expression from Lun et al. for the solid bulk viscosity.)

Figure 4 shows the influence of different models for estimating the solid bulk viscosity. It is seen that, within the range of our investigations, the solid bulk viscosity almost has no effect on simulated results. Therefore, a zero value is assigned to the solid bulk viscosity in most of our subsequent simulations.

Restitution coefficient

The restitution coefficient is varied from 0.81 to 0.99 to study its effect on the simulation result. Comparing with the base case with e_{ss}=0.9, a 10% increase of the restitution coefficient affects significantly on simulated results. On the other hand, a 10% decrease of the restitution coefficient has almost no effect on the distribution of the static pressure and the axial solid velocity. A value of 0.9, which is the typical value used in most simulations in the literature for glass bead particles, is thus chosen and used in the simulations throughout this work.

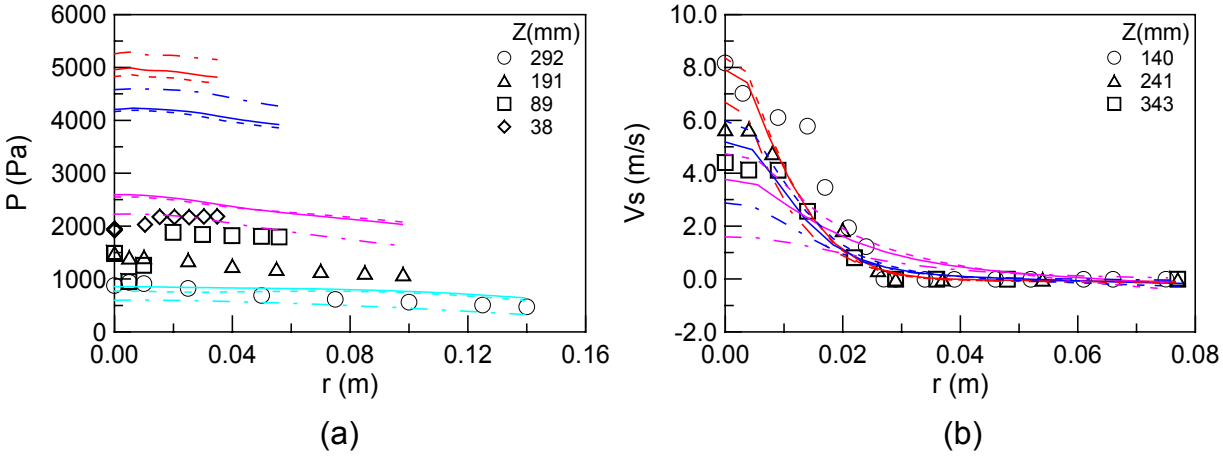

Fig. 5. Comparison between experimental results and simulated results with different restitution coefficient at k_a=1.0 (k_s=1.0, 1/7th power law). Symbols are experimental results, and lines are simulated results. (Solid lines correspond to e_{ss}=0.9, dashed lines correspond to e_{ss}=0.81, dotted dash lines correspond to e_{ss}=0.99.)

The fluid-solid exchange coefficient

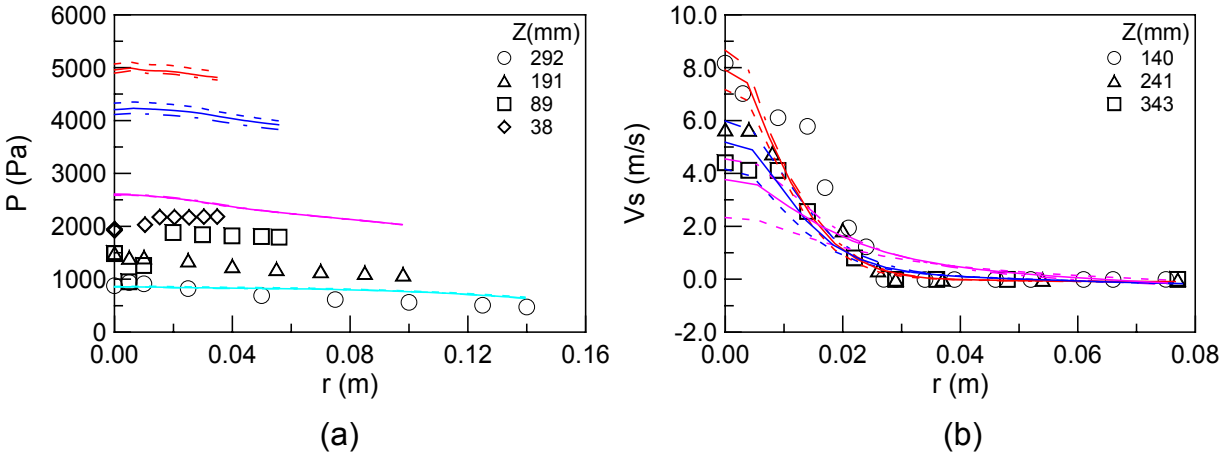

Fig. 6. Comparison between experimental results and simulated results with different fluid-solid exchange coefficient at k_a=1.0 (k_s=1.0, 1/7th power law). Symbols are experimental results, and lines are simulated results. (Solid lines correspond to the fluid-solid exchange coefficient K_{sl} from Gidaspow drag model, dashed lines correspond to 80% of K_{sl}, dotted dash lines correspond to 120% of K_{sl}.)

Figure 6 shows the effect of the fluid-solid exchange coefficient. Within the range of variation, there is little influence of the drag coefficient on profiles of the static pressure, although there is a significant effect on the axial solids velocity distribution. The Gidaspow drag model appears to be a good choice for estimating the fluid-solid exchange coefficient, and was used throughout this study.

The axial solid phase source term

It is seen from figures 2 to 6 that the base case setting of the CFD code with proper inlet velocity profiles, grid size, and parameters on solids bulk viscosity, restitution coefficient and interphase exchange coefficient can properly capture the radial particle velocity distribution profiles in the conical spouted bed. However, variations of these key parameters failed to bring the simulation results close to the static pressure profiles. As pointed at the beginning of the paper, the annulus region in the spouted bed cannot be treated as a fluidized bed, and a source term needs to be introduced to correct the gravitational term in the vertical momentum balance equation for the particle phase. The effect of the solids source term on static pressure and axial particle velocity profiles are simulated based on equations (18) and (19), with the simulation results shown in Fig. 7. It is seen that the axial solid phase source term has a significant impact on the static pressure profile, but has very little effect on the distribution of the axial solid velocity. Compared to experimental data, a selection of k_a=0.7 seems to give the best agreement with the experimental data on the axial solid velocity, while a slightly smaller value of k_a gives better agreement with the static pressure data (see Fig. 8). Therefore, a single constant value of k_a may not be sufficient for simulating conical spouted beds.

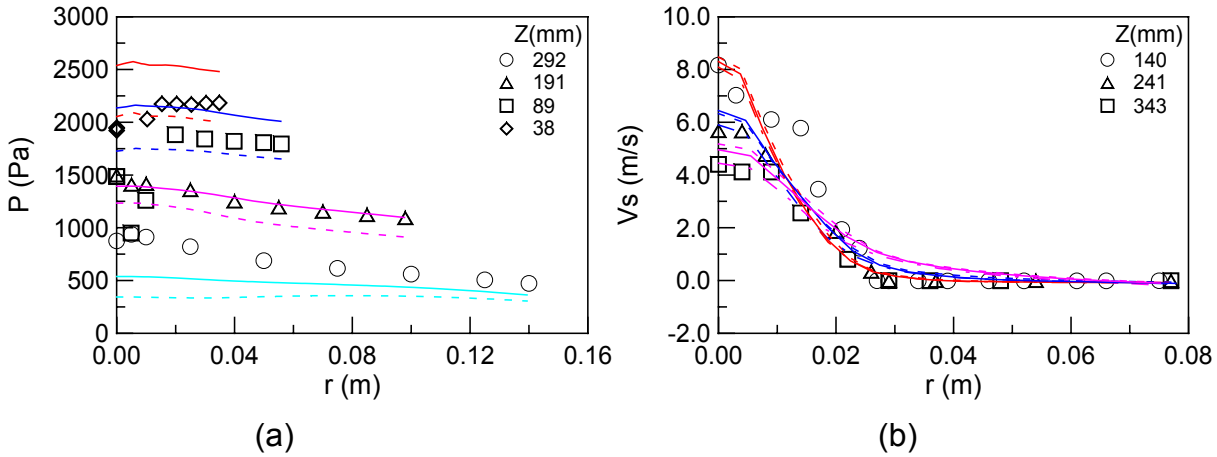

Fig. 7. Comparison between experimental results and simulated results with different axial solid phase source term (k_s=1.0, 1/7th power law). Symbols are experimental results, and lines are simulated results. (Solid lines correspond to k_a=0.5, dashed lines correspond to k_a=0.41, dotted dash lines correspond to k_a=0.7.)

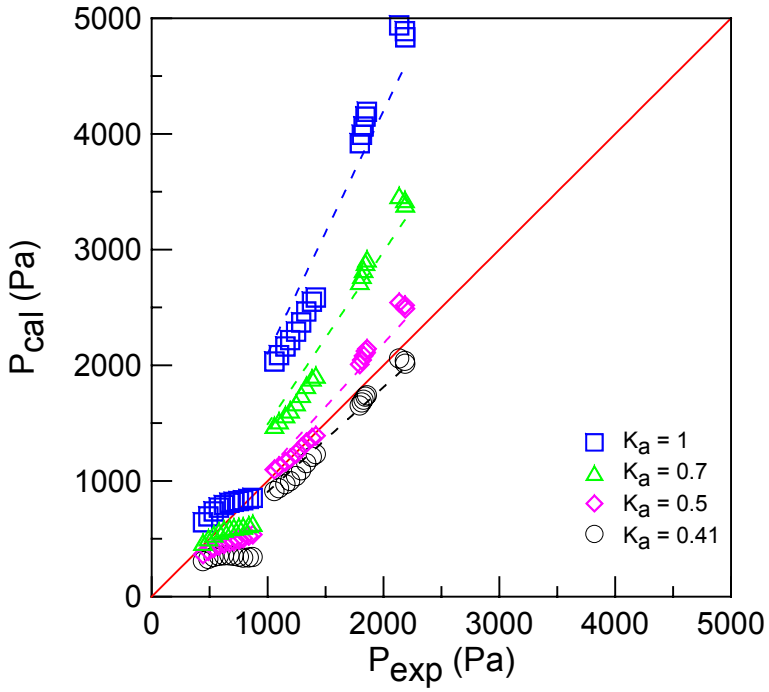

Fig. 8. Comparison between experimental results and simulated results with different axial solid phase source term.

6. Conclusions

Among all factors investigated, the axial solid phase source term has the most significant influence on static pressure profiles, followed by the restitution coefficient, with other factors almost having no effect. Apart from the solid bulk viscosity, almost all other factors affect the distribution of the axial solid velocity, although the effect of the axial solid phase source term is minimal. For a complex system like the conical spouted bed, the introduction of a source term to modify the gravitational force in the annulus region is proven to be essential, although not perfect, in order to give reasonable agreement with the static pressure profile and the particle velocity data.

In the spout region and fountain region, the movement of particles are quite complex, particles were first accelerated from the bed bottom, and then decelerated in the fountain region, thus, the drag force varies a lot in these two dilute regions because of the acceleration and deceleration, while, these two dilute regions are simulated by fluidized beds at dynamic balancing, and the drag force were described by Wen and Yu model (1966). Thus, to simulate these two regions properly, more accurate models for the drag force are needed.

Notations

C_D	drag coefficient
D_0	gas inlet diameter, m
D_c	diameter of the upper cylindrical section, m

D_i diameter of the bed bottom, m

d_s particle diameter, m

e_{ss} restitution coefficient

f drag function

$\vec{g}$ gravitational acceleration, in axial direction, the value is g=-9.81 m/s^2; in radial direction, the value is zero

$g_{0,ss}$ radial distribution function

H_0 static bed height, m

k_a the ratio of the pressure drop of spouted beds to the pressure drop at stable fluidization in the annulus region

K_{ls}=K_{sl} the momentum exchange coefficient between fluid phase *l* and solid phase *s*

k_s the ratio of the pressure drop of spouted beds to the pressure drop at stable fluidization in the spout and fountain region

n total number of phases

P static pressure, Pa

P_{cal} simulation results on the static pressure, Pa

P_{exp} experimental data on the static pressure, Pa

P_s solid pressure, Pa

r radial position, m

Re_s relative Reynolds number

$\vec{S}_s$ solid phase source term

$S_{s,a}$ axial solid phase source term

t time, s

U_i superficial gas velocity based on D_i, m/s

$\vec{v}_q$ velocity of phase q, q can be fluid phase *l* or solid phase *s*, m/s

V_s axial particle velocity, m/s

Z axial height of the bed, mm

Greek letters

α_q volume fraction of phase q, q can be fluid phase l or solid phase s

$\alpha_{l,0}$ loose-packed voidage

$\alpha_{s,0}$ initial solid packing

$\alpha_{s,max}$ packing limit

Θ_s the granular temperature

γ included cone angle, degree

λ_q bulk viscosity of phase q, q can be fluid phase l or solid phase s, kg/(m·s)

μ_q viscosity of phase q, q can be fluid phase l or solid phase s, kg/(m·s)

$\mu_{s,col}$ solid collisional viscosity, kg/(m·s)

$\mu_{s,fr}$ solid friction viscosity, kg/(m·s)

$\mu_{s,kin}$ solid kinetic viscosity, kg/(m·s)

ρ_l gas density, kg/m^3

ρ_s particle density, kg/m^3

$\overline{\overline{\tau}}_l$ fluid phase stress-strain tensor

$\overline{\overline{\tau}}_s$ solid phase stress-strain tensor

τ_s particulate relaxation time

Acknowledgements

This work is supported by the Natural Sciences and Engineering Research Council of Canada (NSERC) under the Discovery Grant program.

References

Aguado, R.; Olazar, M.; San Jose, M. J.; Aguirre, G.; Bilbao, J., “Pyrolysis of sawdust in a conical spouted-bed reactor. Yields and product composition”, Ind. Eng. Chem. Res., 39(6), 1925-1933 (2000a).

Aguado, R.; Olazar, M.; Barona, A.; Bilbao, J., “Char-formation kinetics in the pyrolysis of sawdust in a conical spouted bed reactor”, J. Chem. Technol. Biotechnol., 75(7), 583-588 (2000b).

Duarte, C. R.; Murata, V. V.; Barrozo, M. A. S., “A study of the fluid dynamics of the spouted bed using CFD”, Brazilian Journal of Chemical Engineering, 22(2), 263-270 (2005).

Ergun, S., “Fluid Flow through Packed Columns”, Chem. Eng. Prog., 48(2), 89-94 (1952).

Fluent Inc., “FLUENT 6.1 UDF Manual” (2003a)

Fluent Inc., “FLUENT 6.1 User's Guide” (2003b)

Gidaspow, D., “Multiphase flow and fluidization: Continuum and kinetic theory descriptions”, Academic Press, London (1994).

Goldschmidt, M. J. V.; Kuipers, J. A. M.; van Swaaij, W. P. M., “Hydrodynamic modelling of dense gas-fluidized beds using the kinetic theory of granular flow: effect of coefficient of restitution on bed dynamics”, Chem. Eng. Sci., 56(2), 571-578 (2001).

He, Yurong; Zhao, Guangbo; Bouillard, Jacques; Lu, Huilin, “Numerical simulations of the effect of conical dimension on the hydrodynamic behaviour in spouted beds”, Can. J. Chem. Eng., 82(1), 20-29 (2004).

He, Y.-L.; Qin, S.-Z.; Lim, C. J.; Grace, J. R., “Particle velocity profiles and solid flow patterns in spouted beds”, Can. J. Chem. Eng., 72(4), 561-568 (1994a).

He, Y. L.; Lim, C. J.; Grace, J. R.; Zhu, J. X., “Measurements of voidage profiles in spouted beds”, Journal of Chemical Engineering, 72(2), 229-234 (1994b).

Huilin, L.; Yongli, S.; Yang, L.; Yurong, H.; Bouillard, J. “Numerical simulations of hydrodynamic behaviour in spouted beds”, Chemical Engineering Research and Design, 79(A5), 593-599 (2001).

Kawaguchi, T.; Sakamoto, M.; Tanaka, T.; Tsuji, Y., “Quasi-three-dimensional numerical simulation of spouted beds in cylinder”, Powder Technology, 109(1-3), 3-12 (2000).

Kucharski, J. & Kmiec, A., “Hydrodynamics, heat and mass transfer during coating of tablets in a spouted bed”, Can. J. Chem. Eng., 61(3), 435-439 (1983).

Lu, Huilin; He, Yurong; Liu, Wentie; Ding, Jianmin; Gidaspow, Dimitri; Bouillard, Jacques, “Computer simulations of gas-solid flow in spouted beds using kinetic-frictional stress model of granular flow”, Chem. Eng. Sci., 59(4), 865-878 (2004).

Lun, C. K. K., Savage, S. B., Jeffrey, D. J., and Chepurniy, N., “Kinetic theories for granular flow: Inelastic particles in Couette flow and slightly inelastic particles in a general flowfield", J. Fluid Mech., 140, 223-256 (1984).

Markowski, A. S., “Drying characteristics in a jet-spouted bed dryer”, Can. J. Chem. Eng., 70(5), 938-944 (1992).

Marnasidou, K. G.; Voutetakis, S. S.; Tjatjopoulos, G. J.; Vasalos, I. A., “Catalytic partial oxidation of methane to synthesis gas in a pilot-plant-scale spouted-bed reactor”, Chem. Eng. Sci., 54(15-16), 3691-3699 (1999).

Mathur, K. B. & Epstein N., “Spouted beds”, Academic Press, New York (1974).

McKeen, Tim and Pugsley, Todd, “Simulation and experimental validation of a freely bubbling bed of FCC catalyst”, Powder Technology, 129(1-3), 139-152 (2003).

Mukhlenov, I. P. & Gorshtein, A. E., “Hydrodynamics of reactors with a spouting bed of granular material”, Vses. Konf. Khim. Reactrom Novosibirsk, (3) 553-562 (1965).

Mukhlenov, I. P. & Gorshtein, A. E., “Hydraulic resistance of a fluidized layer in a cyclone without a grate”, Zh. Prikl. Khim., 37(3), 609-615 (1964).

Olazar, M.; Aguado, R.; San Jose, M. J.; Bilbao, J., “Kinetic study of fast pyrolysis of sawdust in a conical spouted bed reactor in the range 400-500 C^{o}”, Journal of Chemical Technology & Biotechnology, 76(5), 469-476 (2001).

Olazar, M.; Aguado, R.; San Jose, M. J.; Bilbao, J., “Performance of a conical spouted bed in biomass catalytic pyrolysis”, Recents Progres en Genie des Procedes, 14(76), 499-506 (2000a).

Olazar, M.; Aguado, R.; Bilbao, J.; Barona, A., “Pyrolysis of sawdust in a conical spouted-bed reactor with a HZSM-5 catalyst”, AIChE J., 46(5), 1025-1033 (2000b).

Passos, M. L.; Oliveira, L. S.; Franca, A. S.; Massarani, G., “Bixin powder production in conical spouted bed units”, Drying Technol., 16(9&10), 1855-1879 (1998).

Passos, M. L.; Massarani, G.; Freire, J. T.; Mujumdar, A. S., “Drying of pastes in spouted beds of inert particles: design criteria and modeling”, Drying Technol., 15(2), 605-624 (1997).

Pham, Q. T., “Behavior of a conical spouted-bed dryer for animal blood”, Can. J. Chem. Eng., 61(3), 426-434 (1983).

Reyes, A.; Diaz, G.; Blasco, R., “Slurry drying in gas-particle contactors: fluid-dynamics and capacity analysis”, Drying Technol., 16(1 & 2), 217-233 (1998).

San Jose, M. J.; Olazar, Martin; Alvarez, Sonia; Izquierdo, Miguel A.; Bilbao, Javier, “Solid cross-flow into the spout and particle trajectories in conical spouted beds”, Chem. Eng. Sci., 53(20), 3561-3570 (1998).

Uemaki, Osamu; Tsuji, Toshiro, “Gasification of a sub-bituminous coal in a two-stage, jet-spouted bed reactor”, in “Fluidization V: Proceedings of the Fifth Engineering Foundation Conference on Fluidization”, Engineering Foundation, New York, 497-504 (1986).

Wen, C. Y.; Yu, Y. H., “Mechanics of fluidization”, Chemical Engineering Progress, Symposium Series, 62(62), 100-111 (1966).

Yang, Ning; Wang, Wei; Ge, Wei; Li, Jinghai, “CFD simulation of concurrent-up gas-solid flow in circulating fluidized beds with structure-dependent drag coefficient”, Chemical Engineering Journal (Amsterdam, Netherlands), 96(1-3), 71-80 (2003).